Available online at www.sciencedirect.com
SCIENCE DIRECT
Journal of Molecular Catalysis A: Chemical 250 (2006) 9–14
JOURNAL OF MOLECULAR CATALYSIS A: CHEMICAL
www.elsevier.com/locate/molcata

Synthesis of SAPO-41 from a new reproducible route using H_3PO_3 as the phosphorus source and its application in hydroisomerization of *n*-decane

Yanfeng Ma [a], Niu Li [b,*], Xingtao Ren [c], Shouhe Xiang [b], Naijia Guan [b]

[a] *Institute of Polymer Chemistry, College of Chemistry, Nankai University, PR China*
[b] *Institute of New Catalytic Material Science, College of Chemistry, Nankai University, Tianjin 300071, PR China*
[c] *Research Institute of Beijing Yanshan Petrochemical Corp. SINOPEC, Beijing 102500, PR China*

Received 19 December 2005; accepted 17 January 2006
Available online 21 February 2006

Abstract

In the new reproducible route, phosphorous acid (H_3PO_3) or the mixture of H_3PO_3 and phosphoric acid (H_3PO_4) are used as the phosphorus source to synthesize microporous silicoaluminophosohates. It is found that gels containing H_3PO_3 favor the formation of SAPO-41 materials. With only H_3PO_3 as the phosphorus source, pure SAPO-41 phase can be prepared with high crystallinity. When the mixture of H_3PO_3 and H_3PO_4 is used as the phosphorus source, the crystallization of SAPO-41 can be accelerated. Raman and XRD results show that SAPO-41 can be formed after crystallizing for 12 h. The dosage of the template di-*n*-propylamine (DPA) can be reduced in the mixed phosphorus source system. The SAPO-41 has been used to prepare catalysts for the hydroisomerization of *n*-decane. High selectivity of isomerization (89.5%) has been observed even at high conversion (88%) over the Pt/SAPO-41.
© 2006 Elsevier B.V. All rights reserved.

Keywords: Phosphorous acid (H_3PO_3); Mixed phosphorus source of H_3PO_3 with H_3PO_4; SAPO-41; Raman; *n*-Decane hydroisomerization

1. Introduction

Hydroisomerization of *n*-paraffins is of considerable interest and plays an important role in the petroleum industry to improve the octane number of gasoline and to increase the low temperature performance of diesel. Catalysts based on molecular sieves with monodimensional non-insecting and medium-pore channels have displayed high selectivity for the task [1–3]. In the family of silicoaluminophosphates, a process for lube dewaxing based on SAPO-11 has been developed [4,5]. It is notable that SAPO-41 has the pore size with 0.70 nm × 0.43 nm and shows very high efficiency for the selective hydroisomerization of long chain alkanes comparing with SAPO-11 (with the pore size 0.39 nm × 0.63 nm) and SAPO-31 (with the pore size 0.54 nm × 0.54 nm) [6]. However, in conventional synthesis route from gels containing phosphoric acid, reactive alumina, silica and organic template di-*n*-propylamine, the pure phase of SAPO-41 is difficult to be reproduced and readily crystallize along with other DPA-templated structures such as SAPO-11 or SAPO-31. Many works contributed to the synthesis of the pure SAPO-41 and AlPO-41 materials have been done in the past few years [7–10]. However, the existence of some difficulties, such as demands of high template concentration, surfactant, high-purity grade reactants or longer crystallizing times, restricted the application of these materials.

Recently, several reports described the usage of non-conventional phosphorus sources. For example, by employing tributylphosphate as the source of phosphorus, several open-framework zinc and cobalt phosphates have been prepared hydrothermally. $Al(H_2PO_4)_3$ or $H_{10}P_8O_{25}$ have been used to the non-fluoride synthesis of triclinic form of $AlPO_4$-34, a CHA-structure type aluminophosphate molecular sieve which has never been synthesized previously in the absence of fluoride ions. Non-conventional phosphorus sources may result in a system with distinct effects for the crystallization of phosphate-based molecular sieves [9,11,12]. The present work reported a new reproducible route to prepare SAPO-41 molecular sieve. By using H_3PO_3 or the mixture of H_3PO_3 and H_3PO_4 as the

* Corresponding author. Tel.: +86 22 23509932.
E-mail address: liniu@nankai.edu.cn (N. Li).

1381-1169/$ – see front matter © 2006 Elsevier B.V. All rights reserved.
doi:10.1016/j.molcata.2006.01.028

P source in the presence of di-*n*-propylamine (denoted as DPA afterwards) as template, the pure SAPO-41 phase has been synthesized in aqueous system. The hydroisomerization of *n*-decane over these Pt/SAPO-41 catalysts showed high selectivity of isomerization (near 90%) even at high conversion (88%).

2. Experimental

2.1. Synthesis of SAPO-41

2.1.1. H_3PO_3 as P source

Pseudoboehmite (2.21 g, water loss at 600 °C: 34.75 wt.%) was mixed with 10 g of deionized water. H_3PO_3 solution (2.87 g of solid phosphorous acid dissolving in 10 g distilled water) was added dropwise to the above mixture to form a white paste. The mixture was stirred until it became homogeneous. Subsequently, 6.98 g of DPA were added dropwise under vigorous stirring. And then 0.6 ml aqueous silica sol (5.9 M SiO_2) and 19.18 g of deionized water were added [13]. The typical molar composition of the reaction mixture is: 0.85 Al_2O_3:2.0 H_3PO_3:0.2 SiO_2:4.0 DPA:95.4 H_2O. The mixture was sealed in a Teflon-lined stainless-steel autoclave and heated at 200 °C under autogenous pressure. The products were filtered, washed with distilled water till pH 7 and then dried at ambient temperature. Table 1 lists the gel compositions and crystallization conditions for the formation of SAPO-41(A). It should be indicated that, the crystallization time in Tables 1 and 2 means the period for obtaining enough solid product to determine its phase and structure. The period of crystallization is from 5 to 9 days according to gel composition and crystallization conditions.

2.1.2. H_3PO_3 and H_3PO_4 as mixed P source

When the mixed P source of H_3PO_3 and H_3PO_4 were used, H_3PO_4 was added following H_3PO_3 according to the molar ratio in Table 2. Take an example (sample 9): 1.43 g of H_3PO_3 was dissolved in 10 ml of distilled water, then 2.28 ml H_3PO_4 was added slowly to H_3PO_3 solution. After stirred for about half an hour, the mixture was added to 2.73 g of pseudoboehmite and then 29.18 g water was added in. The mixture was stirred for 2 h. Then 9.6 ml DPA was added in dropwise under vigorous stirring for 1 h. The typical molar composition of the reaction mixture is: 1.0 Al_2O_3:1.0 H_3PO_3:2.0 H_3PO_4:0.2 SiO_2:4.0 DPA:95.4 H_2O. The mixture was sealed in a Teflon-lined stainless-steel autoclave and heated at 200 °C under autogenous pressure. Table 2 lists the gel compositions and crystallization conditions for the formation of SAPO-41.

2.2. Characterization

X-ray powder diffraction (XRD) patterns of the as-synthesized products were recorded on a Rigaku D/MAX-2500 diffractometer with Ni-filtered Cu Kα radiation (λ = 1.5418 Å). Raman spectra were determined by Renishaw inVia spectroscopy system. The laser used was Argon ion laser with 514.5 nm exitation source with power output of 20 mW. Element analysis was performed on a Elementar Varioel element analyzer. Thermal analysis was performed on Netzsch STA 409 PC thermal analyzer at a heating rate of 10 °C/min in nitrogen.

The acidity of the samples was characterized by temperature-programmed desorption of ammonia (NH_3-TPD). ^{29}Si MAS NMR spectra were recorded at ambient temperature with a BRUKER-AM300 multinuclear spectrometer. Spin speeds

Table 1
Gel compositions and crystallization conditions of SAPO-41

Sample	Reactant composition					Crystallization condition		Product
	Al_2O_3	H_3PO_3	SiO_2	DPA	H_2O	T (°C)	t (day)	
1	0.85	2.0	0.30	4.0	95.4	200	8	SAPO-43
2	0.85	2.0	0.20	4.0	95.4	200	9	SAPO-41
3	0.85	2.0	0.15	4.0	95.4	200	9	SAPO-41
4	0.85	2.0	0.10	4.0	95.4	200	9	SAPO-41
5	0.85	2.0	0.30	3.0	95.4	200	4	SAPO-47
6	0.85	2.0	0.20	3.0	95.4	200	7	SAPO-11
7	0.85	2.0	0.15	3.0	95.4	200	5	SAPO-11
8	0.85	2.0	0.10	3.0	95.4	200	7	SAPO-41

Table 2
Gel compositions and crystallization conditions for SAPO-41 formation with the mixture of H_3PO_3 and H_3PO_4 as the P source

No.	Reactant composition						Crystallization condition	
	Al_2O_3	H_3PO_3	H_3PO_4	SiO_2	DPA	H_2O	T (°C)	Time
9	0.80	0.66	1.33	0.20	2.67	33.33	200	2 days
10	0.80	1.33	0.66	0.07	2.67	33.33	200	4 days
11	0.80	0.66	1.33	0.07	2.67	33.33	200	19 h
12	0.80	0.33	1.67	0.07	2.67	33.33	200	12 h
13	0.80	0.66	1.33	0.07	1.67	33.33	200	2 days
14	0.80	0.66	1.33	0.07	2.67	63.3	200	4 days
15	1.00	0.66	1.33	0.07	2.67	33.33	200	2 days

were ca. 5.5 kHz. The resonance frequencies observed were 79.5 MHz. Chemical shifts were recorded with respect to TMS for ^{29}Si.

2.3. Preparation of Pt/SAPO-41

As-synthesized solid products of SAPO-41(A) were separated from the mother liquor by centrifugation and subsequently purified by a series of washing steps with distilled water, dried at 120 °C for 2 h and then baked in air at 300 °C for 1.5 h. Furthermore, the solid sample was calcined in air by heating at 10 °C/min to 550 °C for 10 h to remove the organic template completely. The composition of the calcined product was determined by inductively coupled plasma (ICP) spectroscopy. Pt/SAPO-41 catalysts were prepared by the incipient wetness impregnation technique. The required amount of an aqueous solution of H_2PtCl_4 was added to the support at room temperature. The metal-loading samples were dried at 110 °C for 2 h and calcined at 500 °C for 4 h. Pt/SAPO-41 based on samples 9 and 11 in Table 2 are designated as SAPO-41-B1 and SAPO-41-B2, the Si/(Si + P) in their framework were 0.09 and 0.05, respectively.

2.4. Catalytic reaction

The *n*-decane hydroisomerization was carried out in a fix-bed continuous flow reactor at atmospheric pressure. The catalyst powder was palletized, sieved to 20–30 mesh and 1.0 g of catalysts were loaded into the reactor. The sample was reduced at 500 °C under hydrogen flow (35 ml/(min g)) for 2 h. After reduction, the temperature was lowered to reaction temperature. Liquid *n*-decane was pumped into vaporization, mixed with hydrogen at 230 °C and fed to the reactor. The reaction products were collected and analyzed by gas chromatograph. The identification of products was done by GC–MS.

3. Results and discussion

3.1. Synthesis and characterization of SAPO-41

3.1.1. Using H_3PO_3 as phosphorus source

Silica and template concentration in the gel have strong influence on the crystallization products. If the molar ratio of SiO_2/H_3PO_3 is greater than 0.1 or DPA/H_3PO_3 less than 1.5, SAPO-41 cannot be obtained. Also, there exists some correlation between silica and template concentration to prepare SAPO-41. Keeping other parameters constant, several DPA-templated SAPO molecular sieves have been obtained by varying silica and template concentration. At higher concentration of template (DPA/H_3PO_3 = 2.0), SAPO-41 have been obtained at a wider range of silica content, the SiO_2/H_3PO_3 molar ratio varying from 0.05, 0.08 to 0.10. When DPA/H_3PO_3 decreased to 1.5, SAPO-41 has only been synthesized at SiO_2/H_3PO_3 = 0.05. ICP analysis show that silica contents in SAPO-41 increase with its feeding.

The powder X-ray diffraction (XRD) patterns of as-synthesized SAPO-41 are shown in Fig. 1. All the reflection peaks of the products can be indexed as SAPO-41, which are in good agreement with the literature values of AFO structure [14]. No additional peaks are observed, which indicates that all the samples are free of impurities. However, the relative intensity of the peaks corresponding to the (2 1 1), (0 2 0) and (2 1 0) planes of sample 2 varied significantly from the literature values, which indicates the different tropism of the products [15].

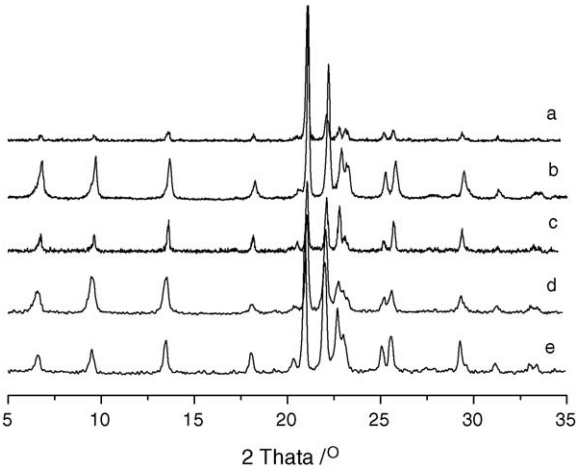

Fig. 1. XRD patterns of as-prepared SAPO-41 samples. (a) Sample 2, (b) sample 4, (c) sample 8, (d) sample 9 and (e) sample 11.

3.1.2. Using the mixture of H_3PO_3 and H_3PO_4 as phosphorus source

Pure SAPO-41 can be prepared by using H_3PO_3 as the phosphorus source, but it needs a long time. In order to shorten the crystallization time, much effort has been done. Finally, a method by using H_3PO_4 partly in place of H_3PO_3 has been discovered.

It is notable that when H_3PO_4 was introduced in the synthesizing procedure, the speed of SAPO-41 formation was accelerated remarkably (Table 2). With other conditions fixed, the crystallization period of SAPO-41 has been reduced from 7 to 9 days in the system H_3PO_3–SiO_2–DPA–H_2O to 2 days in the system H_3PO_4–H_3PO_3–SiO_2–DPA–H_2O. With the changes of H_3PO_4/H_3PO_3 molar ratio from 0.5 to 2 and finally 5, SAPO-41 has even been obtained for about 12–20 h (samples 11 and 12 in Table 2). It is clear that it needs a certain time to perform the transformation of P(III) species to P(V). Introduction of H_3PO_4 to the reaction mixture means reduction of the H_3PO_3 content, so it will take shorter time for the gel to crystallize to SAPO-41.

Besides, by using the mixture of H_3PO_3 and H_3PO_4 as phosphorus source, the dosage of DPA for SAPO-41 formation decreased from DPA/P = 2.0–1.5 with only H_3PO_3 as the P source to 1.3. The molar ratio of DPA/P has even been decreased to 0.8 in Table 2 sample 13.

It has been known that the formation of open-framework structures is kinetically controlled and can be highly sensitive to the variation in reaction conditions such as the choice of solvent, pH and the nature of the metal source [16–19]. In the route using H_3PO_3 as the P source, the formation of SAPO-41 as a preferable product may attribute to the transformation of P(III) species

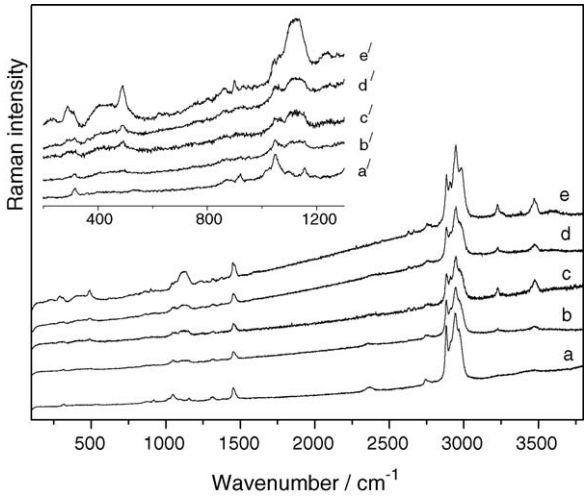

Fig. 2. Raman spectra of the solid gels obtained at various times during the crystallization of SAPO-41 (sample 10). (a)–(e) Correspond to crystallization time of 0, 12, 24, 48 and 72 h, respectively.

to P(V) species in the crystallization procedure. Fig. 2a–e and the corresponding insets a′–e′ show the Raman spectra of the gels obtained as a function of time during the crystallization of SAPO-41 (sample 11). The assignment of the bands (Table 3) has been based on the special work of other researchers [20–26].

The first change in the Raman spectra that should be noted is in the region of 2300–2400 cm^{-1}. This band is assigned to P-H vibration and is characteristic of HPO_3^-. It could be seen that the intensity of this band decrease during the first 12 h, and then disappear after 24 h, which means the P(III) species has transformed to P(V). The initial gel showed Raman bands at 316, 869, 951, 1014 (should), 1026 (should), 1047, 1097 and 1156 cm^{-1} in the region of 200–1300 cm^{-1}. During the crystallization process, some changes can be observed in the Raman spectra. These include decrease in intensity of the 316 cm^{-1} band, appearance and sharpening of the 289 and 491 cm^{-1} band, shift of 921 cm^{-1} band to 898 cm^{-1}, appearance and increase in intensity of the broad band around 1121 cm^{-1}. The band at 491 cm^{-1} is assigned to the motion of the framework oxygen atom in the plane perpendicular to the T–O–T band, and is correlated with the formation of even-numbered rings such as four-rings [25,26]. The band around 1121 cm^{-1} correspond to the stretching vibration of P–O [21,22]. These two bands are first observed around 12 h, which suggests the formation of SAPO-41, and this is in agreement with XRD result. The band in the region of 2700–3000 and 1448 cm^{-1} can be assigned to the C–H stretching and deforming vibration [20–22] of the template DPA.

Table 3
Assignment of vibration bands [20–26]

Wavenumber (cm^{-1})	Assignment
3479, 3226	O–H stretching vibration
2750–3000	C–H stretching vibration
2300–2450	P–H vibration
1448	Deformation vibration of CH_2
850–1200	P–O stretching vibration
350–550	Bending vibration of T–O–T

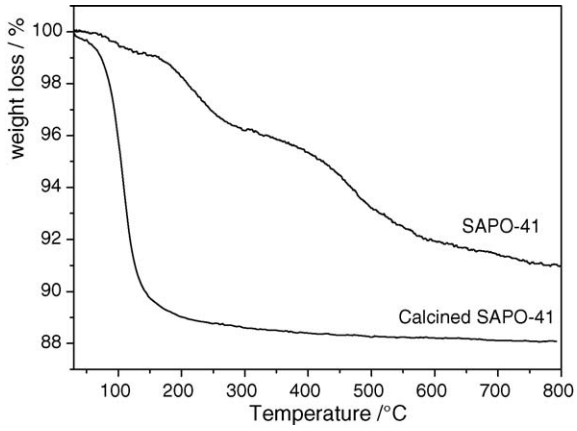

Fig. 3. TGA curves of as-prepared and calcined SAPO-41 (sample 11).

The TGA curve in Fig. 3 of as-prepared SAPO-41 (sample 11) exhibits three weight losses: the first one being about 0.85% occurring from 50 to 140 °C can be assigned to desorption of water molecules. The second weight losses about 2.92% occurring from 140 to 310 °C, and the third about 4.55% appearing between 310 and 645 °C are attributed to the elimination of the template and other organic molecules. TGA curve of SAPO-41 calcined as described in Section 2 exhibits only one weight loss around 100 °C, which suggests that the template in the pores of SAPO-41 has been completely removed.

3.2. Catalytic activity

3.2.1. Acidity of SAPO-41

The catalytic performances of SAPO-*n* molecular sieves are strongly related to their acidity. The acidity of these materials result from the incorporation of silicon into the $AlPO_4$ framework by silicon substituting only phosphorus (mechanism 2) or a phosphorus–aluminum pair (mechanism 3) [27,28].

^{29}Si MAS NMR spectra and temperature-programmed desorption of ammonia NH_3-TPD patterns of SAPO-41 samples are shown in Fig. 4. For sample 11 with lower Si content, a resonance line centered around −91 ppm is observed, which can be ascribed to tetrahedral silicon atoms bound via oxygen to four aluminum atoms by the substitution mechanism 2 [27,6]. Each silicon atom incorporated in this way should produce a Bronsted acid site. For sample 9 with higher Si content, the additional line around −110 ppm is noted, which is assigned to Si atoms linked to neighboring Si atoms by the substitution mechanism 3. Substitution by mechanism 3 will generate much lower acidity than mechanism 2 [28]. So sample 11 should have more acid sites compared to sample 9.

It can be seen from the NH_3-TPD patterns that the amount of NH_3-desorption of sample 11 is much more than that of sample 9, namely, the acid site number of sample 11 is about three times as that of sample 9. This is in accordance with the above result. The two samples with different Si content give a large peak at about 210 °C. This large peak can be assigned to weak acid sites formed by the substitution mechanism 2. For sample 9 with higher Si content, a small shoulder peak around 320 °C

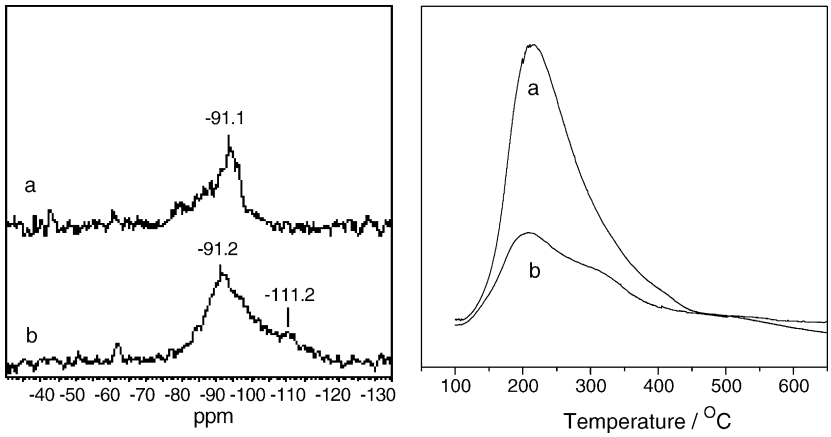

Fig. 4. ^{29}Si MAS NMR spectra (left) and NH_3-TPD patterns (right) of SAPO-41: (a) sample 11 and (b) sample 9.

Table 4
Results of *n*-decane hydroisomerization over SAPO-41 catalysts (in wt.%)

Reaction temperature (°C)	SAPO-41-B1				SAPO-41-B2			
	Conversion (%)	Selectivity of isomers (%)	Yield of isomers (%)	I/C	Conversion (%)	Selectivity of isomers (%)	Yield of isomers (%)	I/C
260	30.7	88.1	27.0	7.4	–	–	–	–
270	44.1	82.3	36.3	4.6	–	–	–	–
280	70.0	80.9	56.6	4.3	26.5	98.5	26.2	67.0
290	84.2	71.0	59.8	2.4	41.6	94.3	39.2	16.5
300	93.8	68.3	64.1	2.2	65.5	92.4	60.5	12.2
310	96.1	65.0	62.5	1.9	84.0	90.5	76.1	9.5
320	–	–	–	–	89.5	88.1	78.8	7.4
330	–	–	–	–	92.3	85.3	78.8	5.7
340	–	–	–	–	93.9	76.7	72.0	3.3

WHSV: 2/h; H_2 flow rate: 35 ml/(min g); weight of catalyst: 1 g; time on stream: 0.5 h; I/C: isomers products/cracked products.

is observed, which is attributed to strong acid sites formed by the substitution of Si for Al and P pairs.

3.2.2. *Catalytic performance of Pt/SAPO-41*

Bifunctional Pt (0.5 wt.%)/SAPO-41 catalysts based on samples 9 and 11, which have different Si content, were tested for the hydroisomerization of *n*-decane. The conversion of *n*-decane and isomers selectivity over Pt/SAPO-41 catalysts at 260–340 °C are shown in Table 4. The Pt/SAPO-41-B showed high isomer selectivity and high I/C value (ratio of isomers products/cracked products) for the hydroisomerization reaction of *n*-decane. High selectivity of isomerization (89.5%) was observed even at high conversion (88%) over Pt/SAPO-41-B2 catalyst. According to Meriaudeau et al. [6], the higher isomerization selectivity of Pt/SAPO-41 catalyst can be considered as a result of its pore dimension which varies the residence time of the reaction intermediates in the channels.

It can be seen from Table 4 that, to achieve high *n*-decane conversion, a higher reaction temperature is required over Pt/SAPO-41-B2 catalyst, which mean it has lower activity than Pt/SAPO-41-B1. But Pt/SAPO-41-B2 catalyst shows higher isomer selectivity and higher I/C value. Based on ^{29}Si MAS NMR and NH_3-TPD analysis, acidity of sample 9 is stronger than sample 11, but the acid site number of sample 11 is greater than sample 9. It is believed that the higher *n*-decane conversion and lower isomer yield over sample 9-based Pt/SAPO-41 catalyst is due to its strong acidity, while the higher isomer yield obtained over sample 11-based Pt/SAPO-41 is due to its suitable number of weak acid sites or suitable silicon content.

4. Conclusions

The present investigation describes the new route to synthesize pure AFO-type SAPO-41 in the presence of phosphorous acid (H_3PO_3). It was found that, SAPO-41 can be obtained in a range of gel compositions, but the crystallization time was somehow as long as 5–9 days. When the mixed phosphorus source of H_3PO_3 and H_3PO_4 were used, the crystallization period of SAPO-41 can be shortened to 20 h–2 days. This is very important and useful for the application of SAPO-41 such as in the hydroisomerization of long-chain paraffin. The Pt/SAPO-41 showed high selectivity for the hydroisomerization of *n*-decane. High selectivity of isomerization (89.5%) was observed even at high conversion (88%) over Pt/SAPO-41-B2.

Acknowledgements

This work was supported by the National Natural Science Foundation of China (NSFC 20473040; 20233030) and National Basic Research Program of China (2003CB615801).

References

[1] L.B. Galperin, Appl. Catal. 209 (2001) 257.
[2] S. Ernst, J. Weitkamp, J.A. Martens, P.A. Jacobs, Appl. Catal. 48 (1989) 137.
[3] P. Meriaudeau, V.A. Tuan, V.T. Ngheim, C. Naccahe, G. Sapaly, Catal. Today 49 (1999) 285.
[4] S.I. Miller, US Patent, 5,135,638 (1992).
[5] S.I. Miller, Microporous Mater. 2 (1994) 439.
[6] P. Meriaudeau, V.A. Tuan, V.T. Nghiem, S.Y. Lai, L.N. Hung, C. Naccache, J. Catal. 169 (1997) 55.
[7] A.K. Sinha, C.V.V. Satyanarayana, D. Srinivas, S. Sivasanker, P. Ratnasamy, Micropor. Mesopor. Mater. 35–36 (2000) 471.
[8] Q. Gao, J. Chen, S. Li, R.R. Xu, Micropor. Mater. 7 (1996) 219.
[9] A. Tuel, S. Caldarelli, A. Meden, L.B. McCusker, C. Baerlocher, A. Ristic, N. Rajic, G. Mali, V. Kaucic, J. Phys. Chem. B104 (2000) 5697.
[10] L. Vidal, C. Pray, J. Patarin, Micropor. Mesopor. Mater. 39 (2000) 113.
[11] S. Neeraj, C.N.R. Rao, A.K. Cheetham, J. Mater. Chem. 14 (2004) 814.
[12] D.A. Lesh, R.L. Patton, N.A. Woodward, Eur. Pat. Appl. 293939.
[13] N. Li, S.H. Xiang, ZL03121112.7.
[14] M.M.J. Treacy, J.B. Higgins, Collection of Simulated XRD Powder Patterns for Zeolites, fourth revised ed., 2001, p. 36.
[15] J. Liang, J. Liu, Q. Xie, S. Bai, W. Yu, Y. Qian, J. Phys. Chem. B 109 (2005) 9463.
[16] R.E. Morris, S.J. Weigel, Chem. Soc. Rev. 26 (1997) 309.
[17] D.A. Bruce, A.P. Wilkinson, M.G. White, A.J. Bertrand, J. Solid State Chem. 125 (1996) 228.
[18] J. Yu, Y. Wang, Z. Shi, R. Xu, Chem. Mater. 13 (2001) 2972.
[19] S. Natarajan, S. Neeraj, A. Choudhury, C.N.R. Rao, Inorg. Chem. 39 (2000) 1426.
[20] A.C. Gujar, A.A. Moye, P.A. Coghill, D.C. Teeters, K.P. Robers, G.L. Price, Micropor. Mesopor. Mater. 78 (2005) 131.
[21] K.H. Schnabel, G. Fingert, T. Kornatowski, E. Löffler, C. Peuker, W. Pilz, Micropor. Mater. 11 (1997) 293.
[22] M. Rokita, M. Handke, W. Mozgawa, J. Mol. Struct. 555 (2000) 351.
[23] S.B. Hong, Micropor. Mater. 4 (1995) 309.
[24] L. Marchese, A. Frache, E. Gianotti, G. Martra, M. Causà, S. Coluccia, Micropor. Mesopor. Mater. 30 (1999) 145.
[25] P.K. Dutta, D.C. Shieh, B.M. Puri, Zeolite 8 (1998) 306.
[26] P.K. Dutta, K.M. Rao, J.Y. Park, J. Phys. Chem. 95 (1991) 6654.
[27] A.M. Prakash, S.V.V. Chilukuri, R.P. Bagwe, S. Ashtekar, D.K. Chakrabarry, Micropor. Mater. 6 (1996) 89.
[28] J.A. Martens, P.J. Grobet, P.A. Jacobs, J. Catal. 126 (1990) 299.